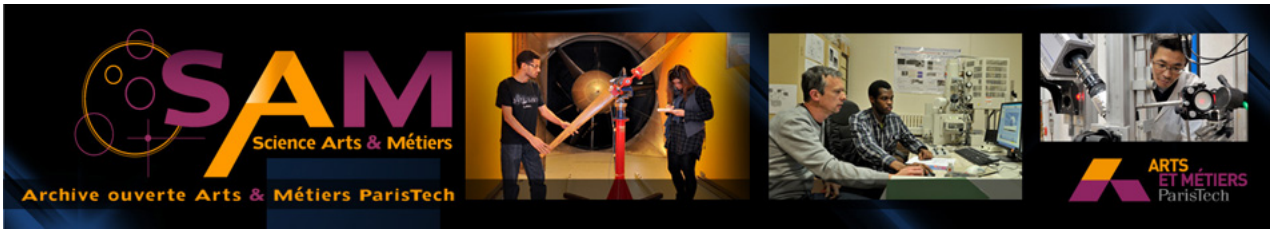

An ageing elasto-viscoplastic model for ceramics

Julian Soulacroix[1,2], Bruno Michel[1], Jean-Marie Gatt[1], Régis Kubler[2], Laurent Barrallier[2]

[1]CEA Cadarache, DEN/DEC/SESC/LSC Bât 151, 13108 St Paul-lez-Durance
[2]MSMP, Arts et Métiers ParisTech, 2 Cours des Arts et Métiers, 13617 Aix en Provence

Abstract

A model reproducing strain softening behavior in ceramic materials is proposed, base on a critical treatment of previous mechanical experimental results on uranium dioxide. The main hypothesis is that the strain softening phenomenon is related to an ageing process, where some point defects move towards the dislocations and modify their velocity. This is different from most of models used up to now, as they were based on the hypothesis that only the initial lack of dislocations was responsible of the strain softening behavior. A model is first developed in a simple 1D framework. Evolution of the mechanical behavior with strain rate and temperature is well reproduced by this model. Then, the 1D model is extended to a 3D mechanical model, and mechanical compressive tests on UO_2 pellets are simulated. The 3D model well reproduces the observed asymmetrical shape of the compressed pellet if one considers that the material is not initially perfectly homogeneous, which highlights the importance of accounting for spatial heteregeneity of materials in models.

Keywords

ceramics, uranium dioxide, strain softening, mechanical behavior, ageing

1 Introduction

Most ceramics are brittle at low and medium temperature and can be deformed plastically only above the brittle-to-ductile transition temperature. This was an important experimental barrier for a long time. It was overcome by Wachtman and Maxwell ([Wachtman and Maxwell, 1954]), and Kronberg ([Kronberg, 1957]), who first developed high temperature mechanical testint techniques and were able to deform samples at temperatures above 1000°C and more. Since this pioneering work, the past decades saw much activity in this field, especially in the experimental study of dislocations in ceramics (a review can be found in [Mitchell and Heuer, 2005]). Despite their high potential, the knowledge of mechanical behavior of ceramics above the brittle-to-ductile transition temperature is still incomplete compared to metals. Particularly, there are few numerical mechanical models of such materials.

In our study, we focus on strain softening behavior, which is a rather common behavior observed in ceramics. This behavior is traduced, during a compressive test at constant strain rate, by a maximum on the stress - strain curve. This was first observed on alkali halides and ionic crystals ([Johnston, 1962, Brown and Pratt, 1963]) (these ceramics can be plastically deformed at ambient or moderated temperature, which makes the tests easier). The main explanation for this behavior was supposed to be the fast multiplication of dislocations at the begining of deformation, due to an initial lack of dislocations, which enventually leads to a softer material ([Gilman, 1961]). This reasonable theory was not directly linked to the yield point and Lüders bands observation in some BCC metals, especially in soft steels ([Friedel, 1964]), even though the two behaviors are extremely close. More recent observations on ceramics, particularly on oxide ceramics such as MnO ([Goretta and Routbort, 1986]), MgO ([Srinivasan and Stoebe, 1973]), UO_2 ([Guerin, 1975, Lefebvre, 1976]) and ZrO_2 ([Tikhonovsky, 2001, Gallardo-Lopez et al., 2004]) have shown that there was a link between strain softening, impurity concentration and strain rate sensitivity. Finally, the lack of dislocations theory can not explain all of the observed behavior, and it needs to be completed. In the present paper, we propose a model that accounts for the effect of strain rate and temperature and clearly highlights the role of defects for such materials. This theory is applicable to ceramics but also to many materials in which strain softening is observed.

In our study, we apply our model to uranium dioxide (UO_2) which is the most used fuel for nuclear power production. At high temperature ($T \gtrsim 1000$°C), the physical cause of the plastic deformation of this material depends on the applied stress. Whereas for very low stress, plasticity is a diffusional phenomenon, the cause of inelastic strain for high stress is dislocations' glide (a full strain mechanisms map can be found in [Frost and Ashby, 1982]).

Uranium dioxide has been extensively studied since the 1960's. Different aspects of its mechanical behavior were studied experimentally and some phenomenological models were then established (see for example [Scott et al., 1959, Armstrong et al., 1962]). These first experiments have shown that UO_2's plastic behavior is sensitive to temperature and strain rate. However, the discrepancies between experimental results has led to the conclusion that UO_2's mechanical behavior is sensitive not only to those two parameters, but also to its chemical composition, such as stoichiometry ([Nadeau, 1969, Burton and Reynolds, 1973]) or impurities concentration ([Christie and Williams, 1962, Armstrong and Irvine, 1964]). More recently, new developments of computing methods allowed to study several aspects of this material numerically. Both macroscopic ([Monerie and Gatt, 2006]) and microscopic ([Sauter and Leclercq, 2003, Pacull, 2011]) mechanical models were developed. There main purpose was to determine a globally consistent model that could be used, for example, in the case of simulating fuel element behavior under operation ([Michel et al., 2008, Michel et al., 2013]). However, some recent studies using molecular dynamics techniques ([Fossati, 2012]) suggest that dislocations are influenced by their nearest chemical environment, such as atomic disorder on oxygen sublattice, which actually confirms the previous experimental statements. The fact that chemical state of this material is deeply modified during irradiation requires a better understanding of the link between phenomena taking place at microscopic or nanoscopic scale, such as diffusion of defects, and macroscopic behavior. This generalizes to other ceramics or materials whose behavior is modified by such microscopic interactions.

Plastic behavior of crystal materials, especially metals, has been extensively studied and modeled. Most of the theories developed for metals also apply to uranium dioxide, but at high temperature and high strain rate only (see [Frost and Ashby, 1982]). A well known

mechanism for metals is the interaction between dislocations and point defects which are in the material, such as precipitates or solute atoms for example (note that the defects can also be created by the plasticity mechanism itself). These mechanisms have been known for decades ([Cottrell and Bilby, 1949, Mura et al., 1961, Bullough and Newman, 1970]). A mechanical theory related to these mechanisms, also called dynamic strain ageing, which was developed during the early 1990's ([McCormick, 1988, Kubin and Estrin, 1990, Estrin and Kubin, 1991]), has shown that Portevin-Le Chatelier (PLC) effect is a direct consequence of this interaction between point defects and dislocations. This kind of model is now very frequently used, and it has recently given good results for modeling the Portevin-Le Chatelier effect during monotonic tensile tests ([Mazière and Dierke, 2012]), and cyclic hardening ([Chaboche et al., 2013]), for example. Such mechanisms can also occur in ceramics, and they were recently indeed identified in cubic zirconia ([Tikhonovsky, 2001, Gallardo-Lopez et al., 2004]) whose crystal structure and mechanical behavior are close to UO_2. PLC effect was also observed in UO_2 ([Yust and McHargue, 1969]), but this is not a common behavior for this material as, to the best of our knowledge, this was only observed once. In this article, we use the same type of theory than for PLC effect, but we show that it mainly manifests by a strong strain softening and a modification of strain rate sensitivity of the material.

Numerical modeling of strain softening may be troublesome: as pointed out in [Engelen et al., 2003], in the case of rate independent behavior, the numerical solution that is obtained from finite element analyses employing standard continuum elasto-plasticity, where a local description of the softening material is used, reveals a pathological dependence on the direction and the fineness of the finite element mesh ([Pijaudier-Cabot et al., 1988]). Accordingly, upon mesh refinement no convergence to a physically meaningful solution exists. A solutions to this problem can be a non-local or gradient enhanced formulation (see for example [Peerlings et al., 2001, Engelen et al., 2003]), which is an efficient method. Another solution is a viscous regularization of the problem ([Needleman, 1988, Borst, 2001]): for a strain rate dependent behavior, strain softening does not always lead to an ill-posed problem. In the case of uranium dioxide, mechanical behavior is actually rate dependent. For this reason, we only developed a local approach of this material's behavior.

In the present paper, we firstly give a new vision of previous experimental mechanical results on UO_2 and discuss the different physical possible explanations for the observed behavior of this material. The second part is the presentation of a new 1D model that was constructed to reproduce the experimental data. Some parameters were fitted to a set of experiments. Finally, a 3D model is presented, which is an extension of the 1D model, and simulations of a compressed pellet are presented. A special point is made on the shape and localization of strain.

2 Experimental overview

2.1 Description of the typical thermomechanical behavior

As uranium dioxide is not totally pure, and fabrication process and test conditions strongly influence its mechanical behavior, there exist some discrepancies between experimental results. This can be explained by slight deviations of stoichiometry ([Nadeau, 1969, Burton and Reynolds, 1973, Keller et al., 1988a, Keller et al., 1988b, Mitchell and Heuer, 2005]), density ([Armstrong et al., 1962, Seltzer et al., 1971]), grain size ([Seltzer et al., 1971, Vivant-Duguay, 1998]) or impurities and addition elements

([Christie and Williams, 1962, Armstrong and Irvine, 1964]). However this material can be characterized by a typical mechanical behavior, which is observed in most of experiments. The following results are obtained after compressive tests on fuel pellet (small cylinder) or single crystal, under imposed strain rate, where both ends are blocked (fig. 1).

1. Strain softening, which leads to a drop of flow stress: this phenomenon is growing (or even appearing) with increasing strain rate, and decreasing temperature ([Guerin, 1975]). This strain softening is repeated after a given ageing time ([Lefebvre, 1976], as seen in fig.2). This behavior seems to be particularly characteristic of fluorite type ceramics ([Tikhonovsky, 2001, Gallardo-Lopez et al., 2004]).

2. Temperature sensitivity of yield stress: under imposed strain rate, the evolution of yield stress as a function of temperature typically exhibits a small plateau ([Guerin, 1975]). An inverse evolution (yield stress growing with increasing temperature) can even be observed for single crystal ([Lefebvre, 1976, Yust and McHargue, 1969], as seen in fig.3).

3. Strain rate sensitivity: under imposed temperature, strain rate sensitivity can be very low for a precise strain rate range. In some cases ([Guerin, 1973]), a higher flow stress can be obtained for a lower strain rate.

4. Localized deformation: as the localized deformation is classical for single crystals, this phenomenon can be obtained at a macroscopic scale during a fuel pellet compressive test. In some cases, the deformation occurs in a asymmetric shape (fig.4), which can not be correlated to any particular non symmetric loading. The localized deformation only appears when a very important strain softening is also observed. As strain softening is well known to produce a localized deformation, this result is not surprising ([Poirier, 1980]).

5. Portevin-Le Chatelier Effect (PLC). PLC effect is rarely observed during compressive tests of uranium oxide, but it has however been observed by Yust et al. ([Yust and McHargue, 1969]). PLC effect is classically observed for some other fluorite type ceramics ([Gallardo-Lopez et al., 2004]).

An important aspect is that all these phenomena are related. For example, at a given strain rate, the temperature for which yield drop appears is the same than the one for which the evolution of yield stress as a function of temperature typically exhibits a small plateau, and than the one for which strain rate sensitivity is strongly reduced.

2.2 Discussion

Some previous models attributed strain softening to an initial lack of dislocations ([Gilman, 1961, Johnston, 1962, Bell and Bonfield, 1964]). As ceramics do not present a high initial dislocation density, and this type of model can indeed reproduce a yield drop for a dislocation-free material (but not for an already deformed material), this hypothesis was occasionally used until recently. For uranium dioxide, this theory was used in several mechanical models ([Pacull, 2011, Sauter and Leclercq, 2003]).

However, this theory can not explain three phenomena: the repeated yield drop and its relation with ageing time, the temperature sensitivity of yield stress and the strain rate sensitivity evolution with strain rate and temperature. As initial dislocation density is not

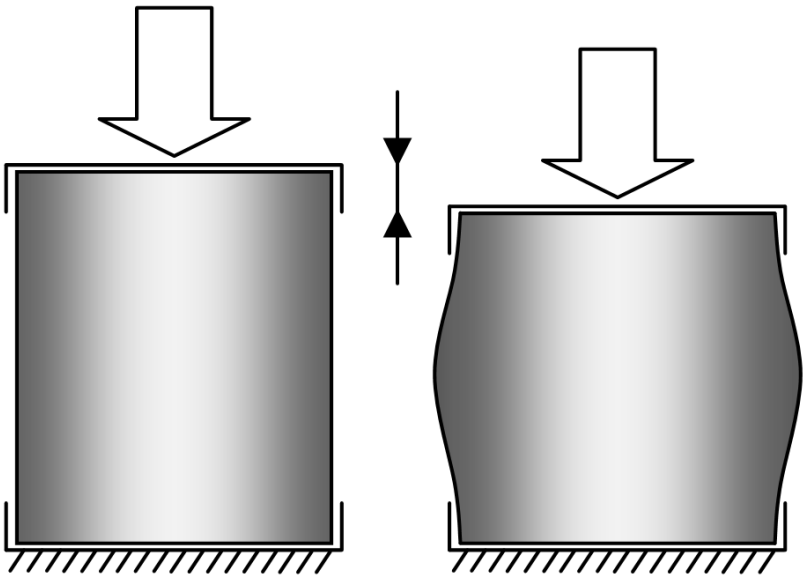

Figure 1: Schematic view of the classical compressive test performed on UO_2 pellets

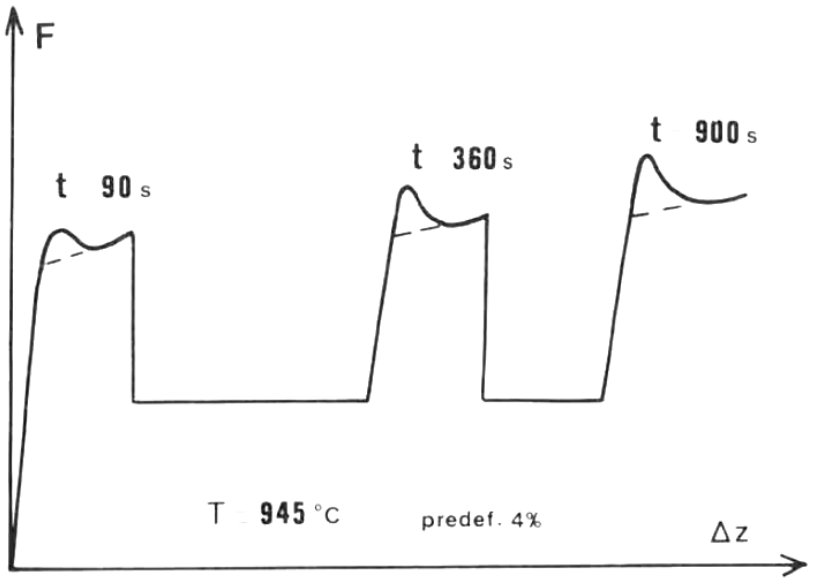

Figure 2: Repeated yield drops for a UO_2 single crystal during a compressive test under imposed strain rate, after [Lefebvre, 1976]. Δz represents the crosshead displacement and F is the measured force. Waiting time is given above each part of the curve, and the three different curves are arbitrarily spaced.

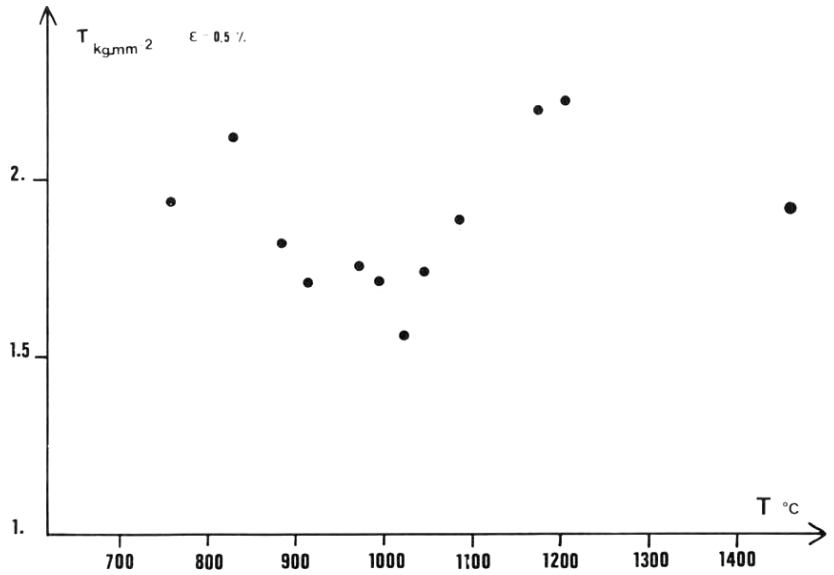

Figure 3: Temperature dependence of yield stress in UO_2 single crystals, after [Lefebvre, 1976]

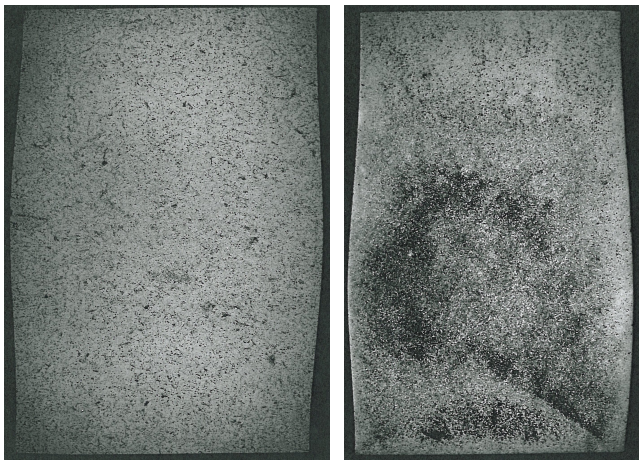

(a) (b)

Figure 4: Cross-section view of an UO_2 pellet after a compressive test at 1500°C under a constant strain rate of $2.7 \cdot 10^{-4} s^{-1}$. Deformation can be symmetric (a) or asymmetric (b) (tests performed at CEA)

easily related to fabrication process or chemical composition, this theory can not explain either the case when yield drop is not observed.

As a result, the observed phenomena should be explained by an interaction between dislocation and some defects. As the strain softening behavior is related to a waiting time during which no deformation occurs and dislocations hence do not glide ([Lefebvre, 1976]), the point defects must be mobile. This excludes some barriers, such as dislocation forest, Lomer-Cottrell locks, or precipitates. However, the precise nature of the main migrating defects in UO_2 is not known. It could be vacancies, solute atoms or any other possible defect.

For all these reasons, we used a simplified dynamic strain ageing theory based on [McCormick, 1988, Kubin and Estrin, 1990, Estrin and Kubin, 1991]. The main hypothesis is that some defects are attracted by dislocations (this process will be simply called ageing throughout this paper). Therefore, dislocations are slowed down by these defects. We will show in the next section, that the proposed model can explain the phenomena previously described, including strain softening, effects of temperature and strain rate, temperature sensitivity of the yield stress and strain rate sensitivity. Contrary to other dynamic strain ageing models, it can not although reproduce the Portevin - Le Chatelier effect.

3 Macroscopic 1D model

3.1 Constitutive equations

3.1.1 Kinematics of the problem

In this one dimension model, strain and stress only have one dimension. Total stress ε_{tot} is assumed to be the sum of two parts: an elastic strain ε_{el} and a viscoplastic strain ε_{vp}: $\varepsilon_{tot} = \varepsilon_{el} + \varepsilon_{vp}$. Stress is linearly related to the elastic strain: $\sigma = E\varepsilon_{el}$. At room temperature, UO_2's Young modulus is about 220 GPa ([Martin, 1989]) and we used this value for all temperatures.

3.1.2 Equation of motion

As suggested by experimental studies (see for example [F. Dherbey, 2002]), in a first approximation, the macroscopic behavior of UO_2 can be simply reproduced by a simple equation:

$$\dot{\varepsilon}_{vp} = \dot{\varepsilon}_0(T) \sinh\left(\frac{|\sigma|}{\sigma_0}\right) sgn(\sigma) \tag{1}$$

where $\dot{\varepsilon}_{vp}$ is the mean viscoplastic strain rate, $\dot{\varepsilon}_0(T)$ the reference strain rate which depends on temperature, σ the stress and σ_0 the reference stress. $\dot{\varepsilon}_0(T)$ and σ_0 are material parameters. The value of $sgn(\sigma)$ is 1 if $\sigma > 0$ and -1 if $\sigma < 0$. This keeps the law consistent for both tension and compression. As for most models, this is only valid for a certain range of temperature and stress (or temperature and strain rate). As pointed out by [Teodosiu, 1976], this quite phenomenological relation is actually closely related to the underlying plastic strain at microscale, which is due to dislocations motion. In this relation, no effect of strain hardening is considered. This is consistent with the experimental results, where very few strain hardening is measured, and it gives a more simple model (see [Guerin, 1973]).

3.1.3 Ageing of dislocations

As previously shown ([Cottrell and Bilby, 1949, Harper, 1951, Mura et al., 1961]), point defects may move towards dislocations and slow them down, or even pin them permanently. If one consider an elementary volume at microscopic scale, containing both defects and dislocations, all dislocations may not be affected simultaneously. For this reason, at a macroscopic scale, we can assume that there exists an ageing stress which will simply slow down dislocations and reduce locally the strain rate for a given applied stress:

$$\dot{\varepsilon}_{vp} = \dot{\varepsilon}_0 (T) \exp\left(-\frac{\sigma_a}{\sigma_0}\right) \sinh\left(\frac{|\sigma|}{\sigma_0}\right) sgn(\sigma) \tag{2}$$

where σ_a is the ageing stress. As shown in [Friedel, 1964], σ_a can be defined as the product of two terms:

$$\sigma_a = \sigma_a^{\infty} c_a(t) \tag{3}$$

σ_a^{∞} is the maximum value of the ageing stress and is related to the nature of interaction between defects and dislocations. c_a is a relative concentration of defects which have moved toward the dislocations and depends upon time (varies between 0 and 1). This concentration is an average over the elementary volume which is considered (this is a mesoscopic parameter). This parameters is the ratio between $N(t)$ (number of defects which have moved toward the dislocations) and N_{max} (maximum number of defects which can move):

$$c_a(t) = N(t)/N_{max} \tag{4}$$

$N(t)$ depends on the waiting time of the dislocations. Although N_{max} is considered as a material parameter in our present model, it could potentially be considered as a variable, because the number of defects depends also on the mechanical history of the material and it can evolve. As the number of dislocations during strain is also changing, the number of defects compared to the number of dislocations may also decrease.

However, if one considers an immobile dislocation, initially free of defects, the number of defects which have migrated after a waiting time t_a is (see. [Quere, 1967]):

$$N(t) = N_{max}\left(1 - \exp\left(-\left(\frac{t_a}{t_0}\right)^n\right)\right) \tag{5}$$

where n is a coefficient between 0 and 1. For long ageing time, we can assume that a saturation phenomenon occurs, and for small times, we have the relation $N(t) \propto t_a^n$. We assume that we have the same relation at the elementary volume scale than for a single dislocation. This finally yields the expression:

$$c_a(t) = \left(1 - \exp\left(-\left(\frac{t_a}{t_0}\right)^n\right)\right) \tag{6}$$

Note that in our model, we use c_a as an internal variable instead of t_a which is more often used, for example in [Estrin and McCormick, 1991]. This change is actually convenient for numerical computation and visualization of the local state of the material. However, one can also invert eq. 6 which gives $t_a = t_0 \left(-\ln\left(1 - c_a\right)\right)^{1/n}$.

The value of n is related the interaction energy between a dislocation line and a moving defect at a distance r. Indeed, if one assumes that the energy is given by the relation:

$$U = \frac{A}{r^{\alpha}} \tag{7}$$

then $n = \frac{2}{\alpha+2}$. For bulk migration of defects, the value of $n = 2/3$ ($\alpha = 1$, which corresponds to an elastic interaction) is commonly used ([McCormick, 1988, Estrin and McCormick, 1991, Kubin et al., 1992]). For pipe diffusion along dislocations, the value of $n = 1/3$ ($\alpha = 4$) was shown to be more consistent ([Ling and McCormick, 1993, Mesarovic, 1995]). For a given material, the value of n can be directly known by measuring the evolution of yield drop with ageing time (see for example [Lefebvre, 1976]). However, the link between the value of measured n and the nature of migration is still not clearly established. For UO_2, ageing experiments have shown a value $n \approx 0.5$ ([Lefebvre, 1976]). However, as the uncertainty of this value is high, a value of $n = 2/3$ can still be considered, and we finally used the $2/3$ value (see tab. 1).

3.1.4 Waiting time of a moving dislocation

For a moving dislocation during a macroscopic stationary deformation, the mean time spent waiting is ([Kubin and Estrin, 1990]):

$$t_w = \frac{\Omega}{|\dot{\varepsilon}_{vp}|} \tag{8}$$

where Ω is a strain increment. For general case, if we consider that only dislocation can stop other dislocations, it has been shown that $\Omega = \rho_m b/\sqrt{\rho_i}$, where ρ_m is the mobile dislocations density and ρ_i is the immobile dislocations density ([Kubin and Estrin, 1990]). In our study, no difference between mobile and immobile dislocations is assumed, which simplifies the problem. We finally have:

$$\Omega = b\sqrt{\rho} \Rightarrow t_w = \frac{b\sqrt{\rho}}{|\dot{\varepsilon}_{vp}|} \tag{9}$$

For our model, as the observed phenomena also appear for prestrained material, when dislocation density changes very little, the dislocation density is approximated by a constant value:

$$t_w = \frac{b\sqrt{\rho_0}}{|\dot{\varepsilon}_{vp}|} \tag{10}$$

A reasonable value of ρ_0 is $10^{13} m^{-2}$, which corresponds to the dislocation density of a sample strained at a few percents [Yust and McHargue, 1969]. A variation of our model with a variable dislocation density (chosen after [Yust and McHargue, 1969]) was tested and did not show any difference on behavior (strain softening, strain rate sensitivity). This validated our hypothesis that dislocation density can be approximated by a constant value.

As used by previous authors (see for example [McCormick, 1988]), we use a first order relaxation time to relate the real ageing time t_a and the stationary ageing time t_w:

$$\dot{t}_a = 1 - \frac{t_a}{t_w} \tag{11}$$

t_a is the real mean waiting time of a moving dislocation. This time is different from the stationary ageing time t_w, because a dislocation cannot age faster than one second per

second. As we chose c_a as an internal variable instead of t_a, we have to express eq. 11 in term of c_a, which finally leads to:

$$\dot{c}_a = \dot{t}_a \frac{\partial c_a}{\partial t_a} = \left(1 - \frac{t_0 \left(-\ln\left(1-c_a\right)\right)^{1/n}}{t_w}\right) \frac{n}{t_0} \left(-\ln\left(1-c_a\right)\right)^{(n-1)/n} \left(1-c_a\right) \tag{12}$$

Note that in a the strain ageing theory, we assume that the evolution of local ageing (c_a in our model), which is a mesoscopic parameter, is still well described by equations given at dislocations scale.

3.1.5 Effect of temperature

The effect of temperature T on the reference strain rate is treated through a heat-activated term:

$$\dot{\varepsilon}_0\left(T\right) = \dot{\varepsilon}_0 \exp\left(-\frac{E_{\mathrm{V}}}{k_B T}\right) \tag{13}$$

where E_{V} is an energy of activation and k_B the Boltzmann's constant. Contrary to FCC metals at room temperature, plasticity in UO_2 in strongly temperature dependent, but no precise mechanism (such as kink pair nucleation on screw dislocations in BCC metals at room temperature for example) has been reported yet in the literature. Some authors attribute this energy to a dislocations core diffusion ([Mohamed and Soliman, 1982]), but this is still an hypothesis.

There also is an effect of temperature on the ageing reference time t_0, which is the time that defects need to saturate the surrounding of a dislocation. According to [Friedel, 1964], this time should be related to temperature with a precise form: $t_0 \propto T \exp\left(\frac{E}{k_B T}\right)$. For our model, our calculations have shown that this type of law underestimates the effect of temperature on ageing. In order to better reproduce experiments, we have finally chosen a phenomenological law:

$$t_0 \propto A \exp\left(-\frac{T}{T_0}\right) \tag{14}$$

3.1.6 Summary of equations and numerical integration

The set of equations can be summarized as follows:

$$\begin{cases} \dot{\varepsilon}_{tot} = \dot{\varepsilon}_{el} + \dot{\varepsilon}_{vp} \\ \varepsilon_{el} = \frac{\sigma}{E} \\ \dot{\varepsilon}_{vp} = \dot{\varepsilon}_0 \exp\left(-\frac{E_V}{k_B T}\right) \exp\left(-\frac{\sigma_a}{\sigma_0}\right) \sinh\left(\frac{|\sigma|}{\sigma_0}\right) sgn(\sigma) \\ \sigma_a = \sigma_a^\infty c_a \\ \dot{c}_a = \left(1 - \frac{t_0(-\ln(1-c_a))^{1/n}}{t_w}\right) \frac{n}{t_0} \left(-\ln\left(1-c_a\right)\right)^{(n-1)/n} \left(1-c_a\right) \\ t_0 = A \exp\left(-\frac{T}{T_0}\right) \\ t_w = \frac{b\sqrt{\rho_0}}{|\dot{\varepsilon}_{vp}|} \end{cases} \tag{15}$$

The parameters are given in tab. 1. This set of differential equations can be seen as a system: $\dot{Y} = F(Y, \dot{\varepsilon}_{tot})$ with $Y = \begin{Bmatrix} \varepsilon_{el} \\ c_a \end{Bmatrix}$. In our code the total strain rate is given as an iterative solution of the non linear static equilibrium problem and controls the evolution of other variables. Viscoplastic strain can be directly deduced from elastic strain: $\varepsilon_{vp} = \varepsilon_{tot} - \varepsilon_{el}$. Stress is also deduced from elastic strain.

The differential equation is solved incrementally. If one knows Y at time t and $\dot{\varepsilon}_{vp}$ is assumed to be a constant between t and $t + \delta t$ (first order approximation), then Y can be known at time $t + \delta t$ using either an implicit scheme or an explicit scheme (for instance Runge-Kutta method). In our model, we tested both and finally used the implicit scheme. In this case, we assume that: $\delta Y = Y(t + \delta t) - Y(t) \approx \delta t \times F(Y + \delta Y, \dot{\varepsilon}_{tot})$. This can be seen as a new equation: $G(\delta Y) = 0$ with $G(\delta Y) = \delta Y - \delta t \times F(Y + \delta Y, \dot{\varepsilon}_{tot})$. The only unknown is δY. The equation was solved using a Newton-Raphson method. This method needs to know the Jacobian term $\frac{\partial G}{\partial \delta Y}$, which we numerically approximated: $\frac{\partial G}{\partial \delta Y} \approx \frac{1}{2\epsilon}\left(G(\delta Y + \epsilon) - G(\delta Y - \epsilon)\right)$ with $\delta Y \gg \epsilon$.

3.2 Physical constants for UO_2

The total number of unknown parameters is low, as there are 3 parameters for global behavior (σ_0, $\dot{\varepsilon}_0$, E_V), and 3 parameters dedicated to ageing process (σ_a^∞, A, and T_0). We used an experimental set of measurements previously obtained at the CEA ([Guerin, 1973], represented on fig. 5) on fuel pellets under compressive stress at imposed strain rate for different temperatures. The 6 unknown parameters were hence adjusted with these experiments (see tab. 1). Fig. 5 shows that our model reproduces the effect of both strain rate and temperature on flow stress and maximum stress, i.e. strain softening.

3.3 Capabilities of 1D model

This model was built to reproduce some special effects, consistent with the mechanical behavior of uranium dioxide. In the simulation, the total strain rate ($\dot{\varepsilon}$) is imposed. Adjusted material coefficients are used (see tab. 1), so that the different plots are consistent with experimental results.

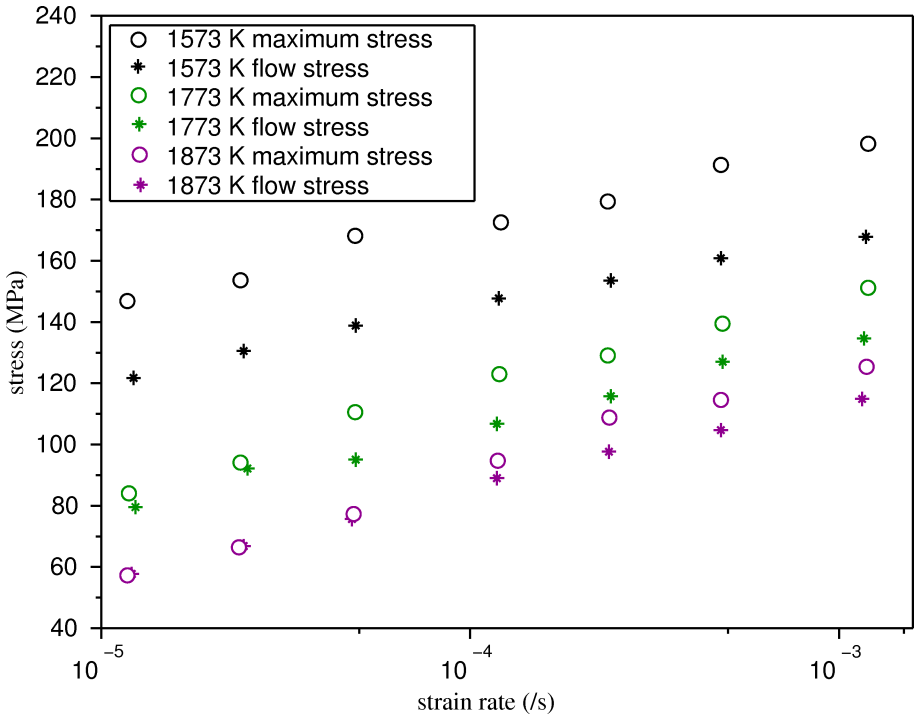

(a)

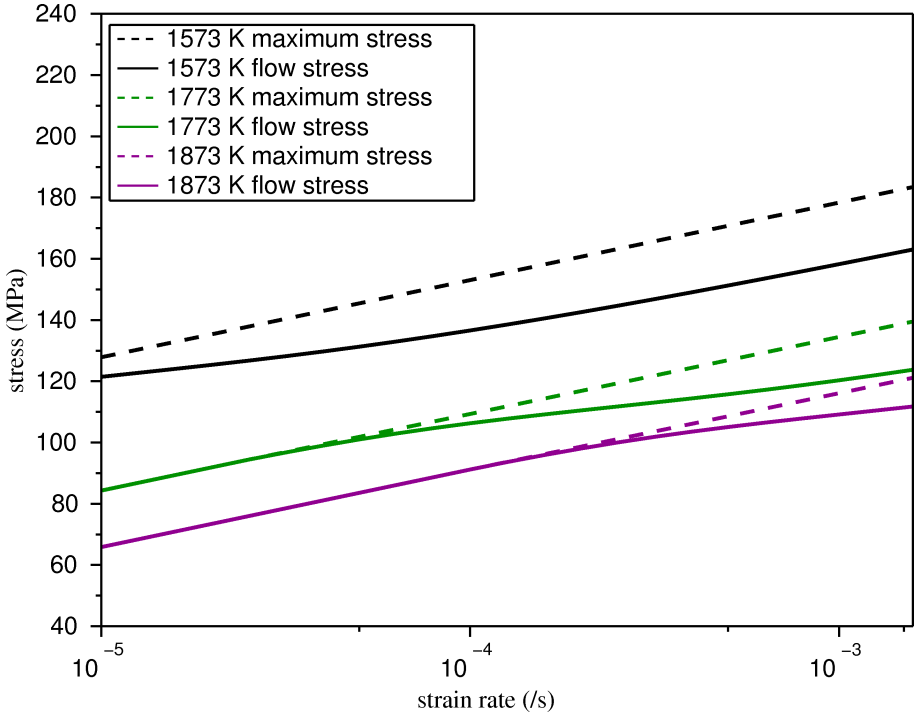

(b)

Figure 5: Comparison between experiments data from [Guerin, 1973] (a) and model (b)

Notation	Parameter	Unit	Value
$\dot{\varepsilon}_0$	Viscoplastic reference strain rate	s^{-1}	3.10^6
b	Burgers' vector length	m	$3.87.10^{-10}$
E_v	Reference energy for dislocations velocity	eV	4.8
σ_0	Reference yield stress	Pa	11
ρ_0	Reference dislocations density	m^{-2}	1.10^{13}
σ_a^∞	Maximum ageing stress	Pa	22
n	Exponent for ageing	-	2/3
A	A material parameter	$s.K^{-1}$	$1.0.10^{-7}$
T_0	Reference temperature for ageing	K	66.6

Table 1: Parameters, units and values used in the model

3.3.1 Strain softening (repeated yield drop)

The initial value of c_a needs to be close to 1 to produce a strain softening effect. Under this condition, the strain-stress curve exhibits a yield drop, which corresponds to the activation of dislocations glide, hence reducing the current ageing concentration and the ageing stress. A low value of $\dot{\varepsilon}_{vp}$ will induce a growing ageing concentration. A new compression test on this aged material will induce a new yield drop (fig 6). Fig. 10 shows that the difference between maximum stress (peak) and flow stress grows with decreasing temperature at given strain rate. The relative size of the peak ($\frac{\sigma_{\text{peak}}-\sigma_{\text{flow}}}{\sigma_{\text{flow}}}$) is illustrated fig. 7. For the chosen temperature and strain rate ranges, it can not exceed a value of 9.1%. It is maximum for a strain rate of $10^{-3}s^{-1}$ (for this strain rate the overstress due to aging, $\sigma_{\text{peak}} - \sigma_{\text{flow}}$, is high) and a temperature of $1650K$ (for this temperature, flow stress σ_{flow} is reduced, due to thermal activation of viscoplasticity). For low strain rate ($10^{-6}s^{-1}$), the relative size of the peak disappears with increasing temperature.

3.3.2 Strain rate sensitivity

Strain rate sensitivity is defined as follows:

$$S = \frac{\partial \sigma^{\text{flow}}}{\partial \ln \dot{\varepsilon}} (\dot{\varepsilon}, T) \tag{16}$$

σ^{flow} here represents the stress that you obtain when you perform a compressive test at a given strain rate $\dot{\varepsilon}$ and given temperature T. Therefore this is not an instantaneous variation of stress with strain rate. For an ageing material, the value of this coefficient is modified by the effect of defects migration. This can lead to a minimum of strain rate sensitivity in the range of temperature and strain rate where dislocations and point defects move with the same speed. For a higher temperature, defects can follow dislocations up to a higher strain rate. This is illustrated by fig. 8 and fig. 9. With our parameters, S is always positive, but fig. 9 clearly shows a valley of low strain rate sensitivity, where it can be as low as 6.8 MPa. This valley corresponds to the strain rate and temperature for which dislocations and point defects move with almost the same speed.

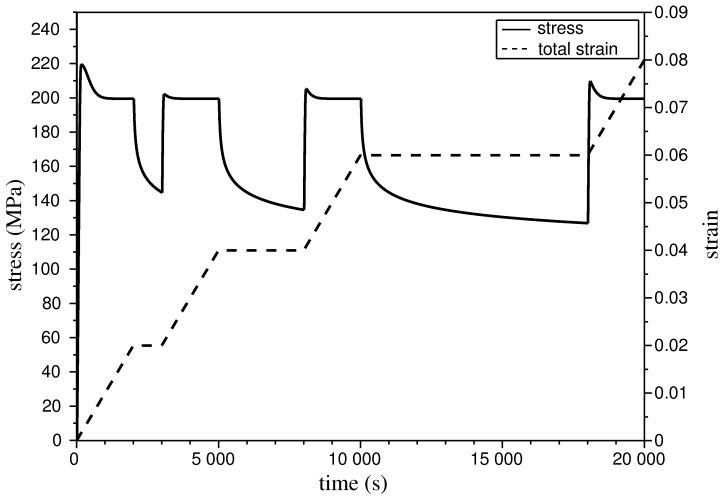

(a)

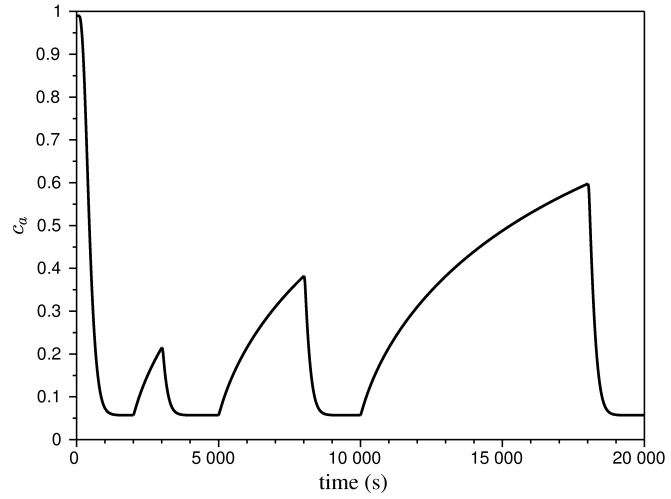

(b)

Figure 6: Evolution of stress and strain (a) and ageing concentration (b) with time for UO_2 at $1273K$. Total strain rate is imposed between $10^{-5}s^{-1}$ and zero (relaxation).

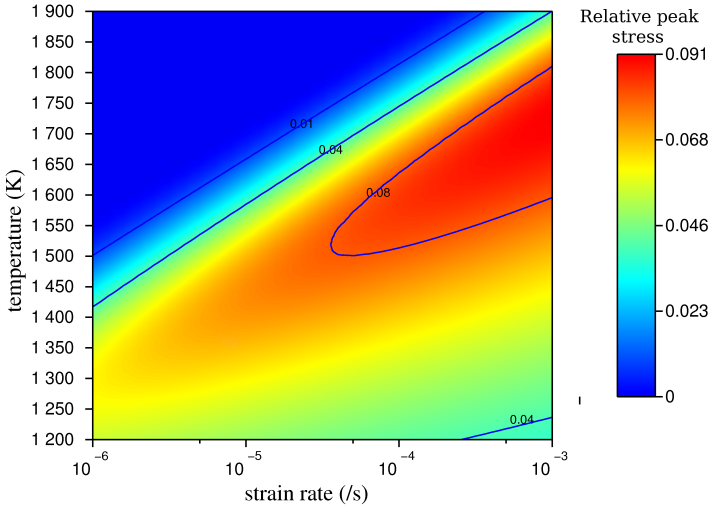

Figure 7: Map of the relative peak stress ($\frac{\sigma_{\text{peak}}-\sigma_{\text{flow}}}{\sigma_{\text{flow}}}$), as a function of temperature and strain rate.

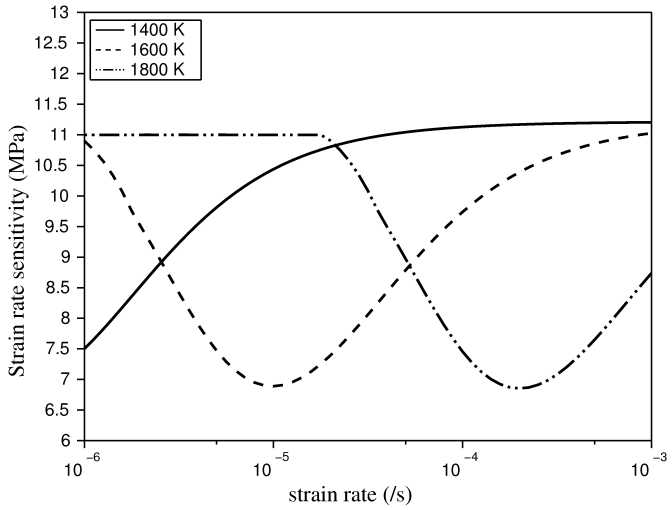

Figure 8: Strain rate sensitivity as a function of strain rate, for different temperatures.

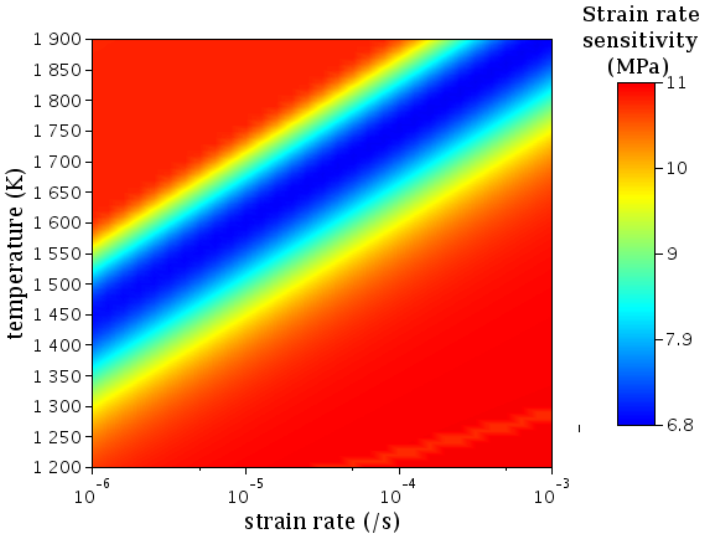

Figure 9: Map of the strain rate sensitivity as a function of temperature and strain rate.

3.3.3 Effect of temperature on yield stress

At a given strain rate, there exists a temperature for which defects and dislocations speeds are approximately the same. In this range of temperature, an increase of temperature will decrease the reference ageing time t_0, hence increasing the ageing stress. The resulting flow stress is therefore decreasing more slowly with temperature(see fig. 10). Fig. 10 also shows that, for a given strain rate, only relatively low temperatures will lead to a compression peak during a test. This peak is greater for lower temperatures, and is disappearing for high temperatures. The temperature delimiting those two regimes is increasing with increasing strain rate, which is consistent with experimental results.

4 3D simulations

4.1 3D constitutive equation

4.1.1 Kinematics of the problem

In this 3 dimensional model, strain and stress are second order tensors. We used a simple small strains formulation. Total stress $\underline{\underline{\varepsilon_{tot}}}$ is the symmetric part of ∇u where u is displacement: $\underline{\underline{\varepsilon_{tot}}} = 1/2\left(\nabla u^T + \nabla u\right)$. $\underline{\underline{\varepsilon_{tot}}}$ is assumed to be the sum of two parts: an elastic strain $\underline{\underline{\varepsilon_{el}}}$ and a viscoplastic strain $\underline{\underline{\varepsilon_{vp}}}$: $\underline{\underline{\varepsilon_{tot}}} = \underline{\underline{\varepsilon_{el}}} + \underline{\underline{\varepsilon_{vp}}}$. This relation can be also written in term of strain rate: $\underline{\underline{\dot{\varepsilon}_{tot}}} = \underline{\underline{\dot{\varepsilon}_{el}}} + \underline{\underline{\dot{\varepsilon}_{vp}}}$. Cauchy stress is linearly related to the elastic strain: $\underline{\underline{\sigma}} = \underline{\underline{\underline{\underline{D}}}} : \underline{\underline{\varepsilon_{el}}}$. At room temperature, UO_2's Young modulus is about 220 GPa and Poisson's ratio is close to 0.3 ([Martin, 1989]), and we used these values for all temperatures.

As any viscoplastic evolution, the viscoplastic flow rule can be written (see [Lemaitre et al., 2009] for more details):

$$\underline{\underline{\dot{\varepsilon}_{vp}}} = \dot{p}\underline{\underline{n}} \tag{17}$$

.

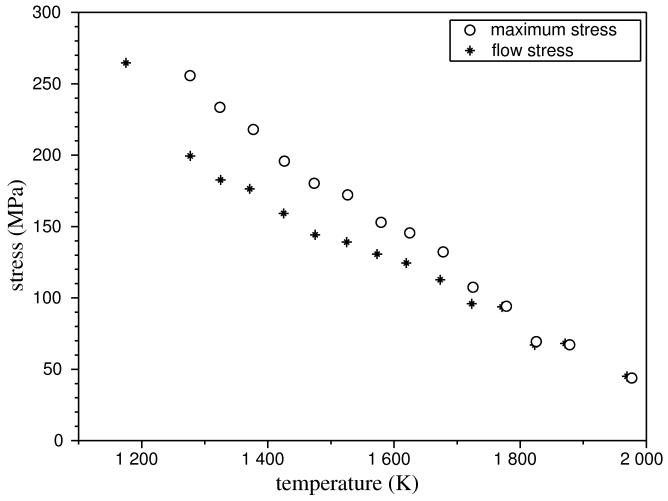

(a)

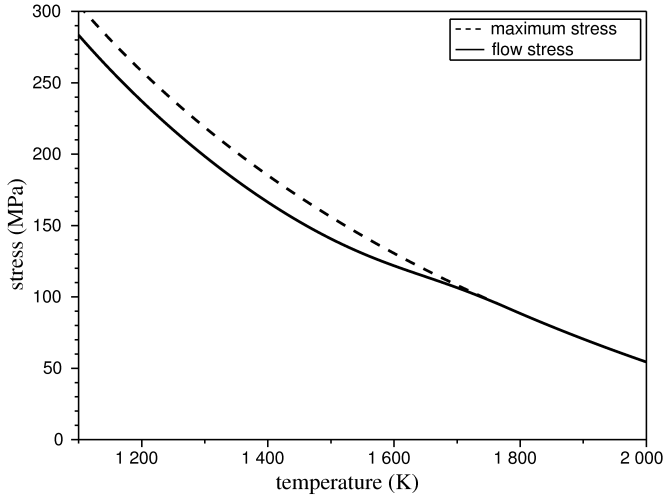

(b)

Figure 10: Evolution of maximum stress and flow stress with temperature for a given strain rate of $2.33 \cdot 10^{-5} s^{-1}$: experiments from [Guerin, 1973] (a) and model (b).

In our model, we used a normal and associated flow, based on von Mises flow potential. In this case, the flow potential Φ only depends on von Mises stress $\sigma_{eq} = \sqrt{\frac{3}{2}\underline{\underline{\sigma}}^D : \underline{\underline{\sigma}}^D}$ (with $\underline{\underline{\sigma}}^D = \underline{\underline{\sigma}} - \frac{1}{3}\mathrm{Tr}(\sigma)\underline{\underline{I}}$):

$$\underline{\underline{\dot{\varepsilon}_{vp}}} = \frac{\partial \Phi\left(\sigma_{eq}\right)}{\partial \underline{\underline{\sigma}}} = \frac{\partial \Phi\left(\sigma_{eq}\right)}{\partial \sigma_{eq}} \frac{\partial \sigma_{eq}}{\partial \underline{\underline{\sigma}}} \tag{18}$$

Thus, $\dot{p} = \frac{\partial \Phi(\sigma_{eq})}{\partial \sigma_{eq}}$ and $\underline{\underline{n}} = \frac{\partial \sigma_{eq}}{\partial \underline{\underline{\sigma}}}$, which can be also written:

$$\underline{\underline{n}} = \frac{3}{2}\frac{\underline{\underline{\sigma}}^D}{\sigma_{eq}} \tag{19}$$

If one chooses $\Phi = \dot{\varepsilon}_0 \exp\left(-\frac{E_\mathrm{V}}{k_B T}\right) \exp\left(-\frac{\sigma_a}{\sigma_0}\right) \cosh\left(\frac{\sigma_{eq}}{\sigma_0}\right)$, this finally gives a result similar to 1D model (eq. 15):

$$\dot{p} = \dot{\varepsilon}_0 \exp\left(-\frac{E_\mathrm{V}}{k_B T}\right) \exp\left(-\frac{\sigma_a}{\sigma_0}\right) \sinh\left(\frac{\sigma_{eq}}{\sigma_0}\right) \tag{20}$$

4.1.2 Finite element formulation

We solved our FE problem with the FE code Cast3M (www-cast3m.cea.fr/). The incremental finite element resolution of non-linear mechanical problems consists in solving at each step i the following problem: assuming a time $t = t^i$, $F_{int}(u^i) = F_{ext}(u^i)$, find the displacement field a time $t = t^{i+1}$, $u^{i+1} = u^i + \Delta u^i$ such as $F_{int}(u^{i+1}) = F_{ext}^{i+1}$. u^i denotes the vector of nodal displacements at step i, and $F_{int}(u^i)$ and F_{ext}^i the corresponding internal and external forces acting on the discretized system. The value of external forces at step $i+1$, F_{ext}^{i+1} is deduced from boundary conditions and loading path. This non-linear problem can be solved at each step using iterative procedures. $\mathbb{B}$ is the shape function derivative matrix. For each calculation iteration k:

1. The displacement field is updated $\Delta u_{k+1}^i = \Delta u_k^i + \delta u_k^i$.
2. The total strain tensor increment at each Gauss point $\Delta\varepsilon_{k+1}^i = \mathbb{B}\Delta u_{k+1}^i$ is computed.
3. The constitutive equations are integrated to provide the internal variables increments (see 4.1.3), including stress increment $\Delta\sigma_{k+1}^i$. Note that we don't compute any consistent tangent operator.
4. Internal forces $F_{int}\left(u^i + \Delta u_{k+1}^i\right)$ are computed.
5. Residual forces $R_{k+1}^i = F_{int}(u^i + \Delta u_{k+1}^i) - F_{ext}^{i+1}$ are computed.
6. The new displacement increment $\delta u_{k+1}^i = -\mathbb{K} R_{k+1}^i$ is computed, where $\mathbb{K}$ denotes the elastic stiffness matrix of the problem (an algorithm can be used at this step to compute another displacement increment which gives a faster convergence).

This iterative process is stopped when $\left|R_{k+1}^i\right| < r$, with r a given small value.

4.1.3 Integration of constitutive equations

We used the same parameters for the 3D model than for the 1D model. Finally, constitutive equations reduce to:

$$\begin{cases} \underline{\underline{\dot{\varepsilon}_{tot}}} = \underline{\underline{\dot{\varepsilon}_{el}}} + \underline{\underline{\dot{\varepsilon}_{vp}}} \\ \underline{\underline{\sigma}} = \underline{\underline{\underline{\underline{D}}}} : \underline{\underline{\varepsilon_{el}}} \\ \underline{\underline{\dot{\varepsilon}_{vp}}} = \dot{p}\underline{\underline{n}} \\ \underline{\underline{n}} = \frac{3}{2}\frac{\underline{\underline{\sigma}}^D}{\sigma_{eq}} \\ \underline{\underline{\sigma}}^D = \underline{\underline{\sigma}} - \frac{1}{3}\mathrm{Tr}(\sigma)\underline{\underline{\mathrm{I}}} \\ \sigma_{eq} = \sqrt{\frac{3}{2}\underline{\underline{\sigma}}^D : \underline{\underline{\sigma}}^D} \\ \dot{p} = \dot{\varepsilon}_0 \exp\left(-\frac{E\mathrm{v}}{k_B T}\right) \exp\left(-\frac{\sigma_a}{\sigma_0}\right) \sinh\left(\frac{\sigma_{eq}}{\sigma_0}\right) \\ \sigma_a = \sigma_a^{\infty} c_a \\ \dot{c}_a = \left(1 - \frac{t_0(-\ln(1-c_a))^{1/n}}{t_w}\right) \frac{n}{t_0} \left(-\ln\left(1-c_a\right)\right)^{(n-1)/n} \left(1-c_a\right) \\ t_0 = A \exp\left(-\frac{T}{T_0}\right) \\ t_w = \frac{b\sqrt{\rho_0}}{|\dot{p}|} \end{cases} \tag{21}$$

The constitutive equations are integrated with the software Mfront which is a tool developed for Cast3M. As Cast3M imposes the total strain tensor increment at each iteration, the basic principle of integration of constitutive equations is strictly the same than the one used in 1D and presented in section 3.1.6 but scalars are replaced by tensors. Therefore, the unknown vector Y is:

$$Y = \begin{Bmatrix} \underline{\underline{\varepsilon_{el}}} \\ c_a \end{Bmatrix} = \begin{Bmatrix} \varepsilon_{el}^{11} \\ \varepsilon_{el}^{22} \\ \varepsilon_{el}^{33} \\ \varepsilon_{el}^{23} \\ \varepsilon_{el}^{13} \\ \varepsilon_{el}^{12} \\ c_a \end{Bmatrix}$$

4.2 3D simulations of the compression of a cylindrical fuel pellet: localization of deformation and effect of heterogeneity

4.2.1 General results

The internal variable c_a, represents the local relative concentration of defects which have migrated to dislocations, and hence represents the local ageing of the material. This internal variable needs to be initialized to perform a simulation. To reproduce a non aged material, c_a will be initialized to a value close to 0, whereas for a well aged material, c_a will be initialized to a value close to 1 (but slightly below 1). As UO_2 is made at a very high temperature (above 1700°C) and slowly cooled to room temperature, the ageing of the material must be close to 1, which means that almost all the point defects which physically can migrate to dislocations have done it.

As shown with fig. 4, UO_2 pellets can deform asymmetrically during a compressive test under imposed strain rate. This phenomenon was studied experimentally in [Guerin, 1975], and it was shown that it could not be explained by the set up of the compressive machine or any asymmetric loading. This asymmetric deformation is strongly related to a great compressive peak during the test: it was never observed for specimens that showed only a small compression peak or even no compression peak.

We simulated a compression test (as represented fig. 1), with the 3D mechanical model and adjusted parameters, for a temperature of 1300°C and a strain rate of $10^{-3}s^{-1}$. Under these experimental conditions strain softening is strong and an asymmetric deformation was occasionally observed ([Guerin, 1975]).

Our simulations have shown that the global behavior of the pellet depends on the initial value of the internal variable c_a and its spatial distribution. This initial field can be spatially homogeneous or heterogeneous.

Case of an initial uniform field: If the initial field of c_a is uniform, the final shape of the pellet is always symmetric (between the two ends of the pellets, and with respect to the central axis of the pellet). This shape is called "barrel shape", and is illustrated at fig. 4 (a). This shape is little dependent on the local mechanical behavior, particularly it does not depend on the occurrence of a local strain softening.

Case of an initial heterogeneous field: If the initial field of c_a is heterogeneous, we observed, in some situations that are explained hereafter, an asymmetric shape of the deformed pellet, very close to the one observed experimentally (see fig. 4 (b)). The deformation process is illustrated fig. 11: the strain rate firstly quickly grows in a precise part of the pellet (closer to one of the ends of the pellets than to the other), then it propagates towards the center of the pellet. The precise position of the first localization seems related to a zone with a lower initial ageing concentration (fig.11), but it is also related to a structural effect of the compressed pellet. Note that the stress - strain curve is not modified by this asymmetric strain, which is the same than for symmetric strain.

4.2.2 Study of effect of heterogeneity on the symmetry of deformation and discussion

There actually are many different ways of introducing and controlling the heterogeneity of the initial field c_a. As there is no physical knowledge of the real distribution of this parameter, we can choose any arbitrary method. In the present work, we generated the initial

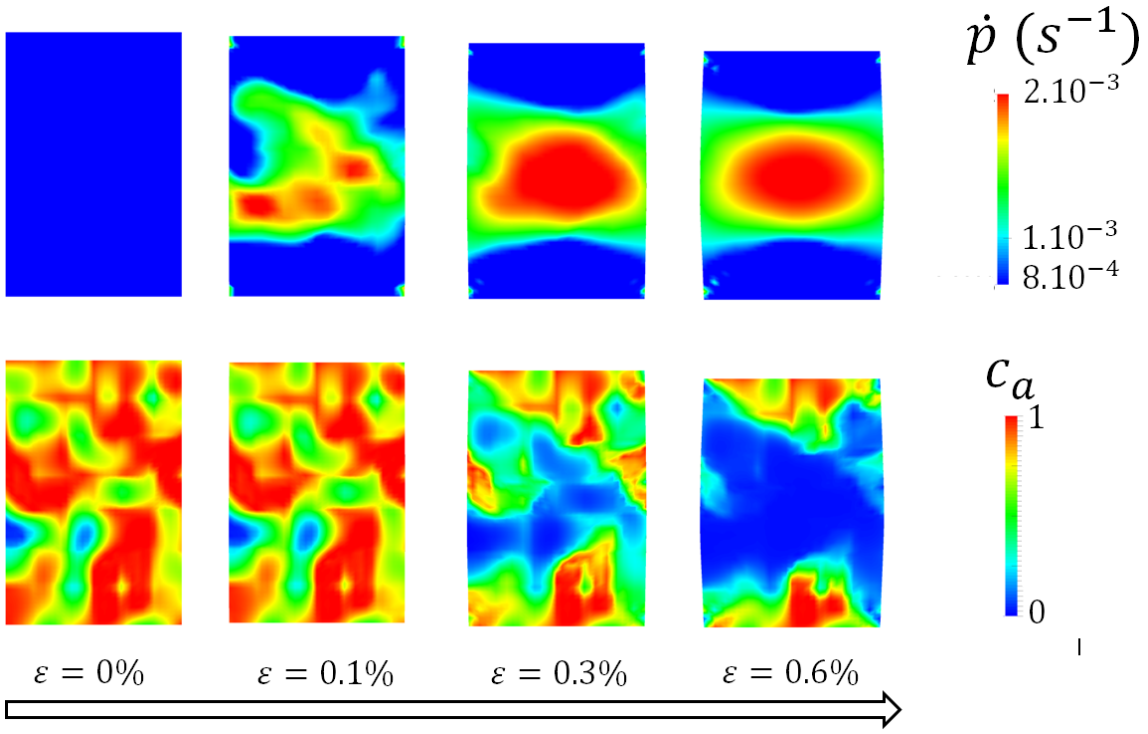

Figure 11: Evolution of localization of strain rate (up) and ageing concentration (bottom) during a compression test with strain rate of $1.10^{-3}s^{-1}$ and temperature of 1200°C, in the case when the final shape of the pellet is slightly asymmetrical. The view is a cut in the pellet so we see the value of the fields inside the sample.

field using a Gaussian probability distribution. This field was generated on a mesh, called "generation mesh" which is different from the mesh used for solving the numerical problem, called "calculation mesh". The c_a field was then projected from generation mesh onto calculation mesh, so the same mechanical problem could be solved with a finer calculation mesh. We then observed the relative position of the maximum strain in the pellet for a macroscopic strain of 0.6% (this value corresponds to the value of h/l of fig. 12): this relative position can be between 0.5 (symmetric localization, i.e. barrel deformation that one obtains if there is no strain softening behavior) and about 0.3 (very asymmetric deformation). We first noticed that this criterion only depends statistically on a given configuration (given generation mesh and probability distribution). Indeed for the same configuration, the real problem which is solved actually depends on the local state of the material, given by the seed used for the pseudo-random generation of c_a field.

In our study, we first generated, on the generation mesh, a distribution of t^* using a Gaussian distribution with parameters s (standard deviation) and μ (expectation) (the probability density function is hence $f(t^*) = \frac{1}{s\sqrt{2\pi}} \exp\left(-\frac{(t^*-\mu)^2}{2s^2}\right)$). Then we calculated the associated c_a values with the formula: $c_a = 1 - \exp\left(-(t^*)^n\right)$. μ hence represents the global ageing of the material: $\mu \gg 1$ means that the material is well aged (c_a is very close to 1). This field was then projected on the calculation mesh. In our simulations, we chose a constant value $\mu = 3$. s represents the heterogeneity of ageing around the mean value. In order to have a global approach of the effect of configuration (given generation mesh and probability distribution) on the position of maximum strain plane, for each configuration, we have computed 400 simulations with varying initial seeds for generating the Gaussian distribution. Our simulations have led to the two following conclusions.

First, if the calculation mesh is finer than the generation mesh, the result of the finite element analysis is mesh independent (this is shown fig. 13). Even if there is a localization of strain, that we can call a shear band, the width of this band is totally independent from the refinement of the calculation mesh. However, the width of the shear band is controlled by the refinement of the generation mesh, but changing the generation mesh actually means changing the initial local state of the material, and then changing the mechanical problem which is solved itself. This approach shows that there is a true mesh independence of our finite element analysis, but there is also a given internal length in our problem, related to the width of shear band, which is given by the initial characteristic length of the local state of the material, i.e. the refinement of the generation mesh. This internal length may also depend on the viscous behavior of the material. We observed that for a very fine generation mesh, the deformation of the pellet tends to be symmetrical, whereas for a rather coarse generation mesh, we have a more frequent asymmetrical deformation (see fig. 14). We think that this characteristic length has a physical meaning, because ceramic materials are often made by a sintering process which cannot ensure that the final material is perfectly homogeneous (porosity or grain size are often varying with the position in the sample). This mesh independence proves that strain softening behavior does not always lead to ill-posed field equations. No non-local or gradient approach was necessary in our case, mostly because we always have a positive strain rate sensitivity due to viscous behavior (see [Needleman, 1988]). However, one has to be very careful with differentiating the mesh used to generate the initial state of the material (and hence determining the problem to be solved) and the mesh used for solving the FE problem. If this step is not achieved, one may deduce incorrect mesh effect.

Secondly, we observed that a higher heterogeneity (i.e. higher standard deviation for

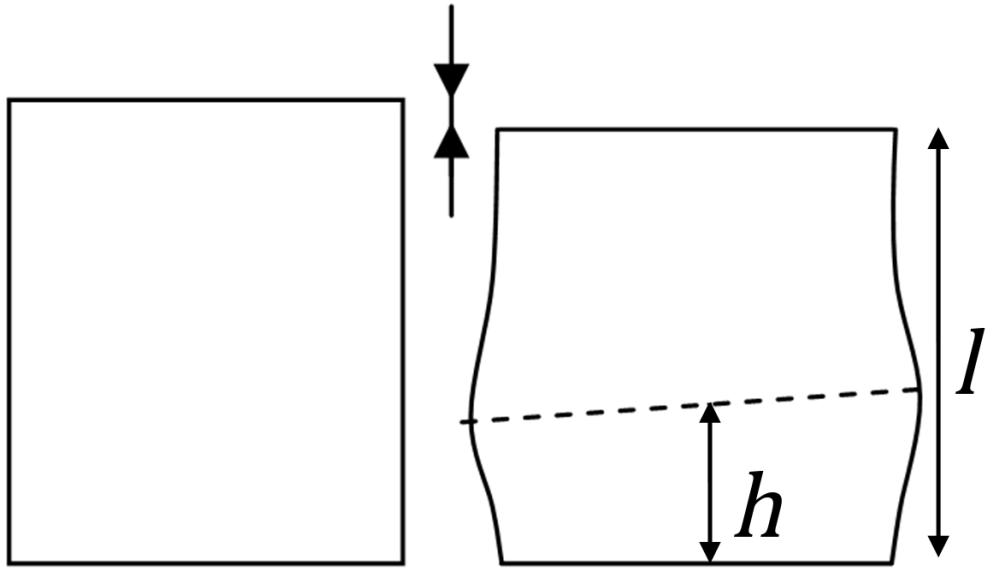

Figure 12: Schematic view of the studied parameter: relative position of the maximum strain plane (localization plane) in the pellet.

the generation of initial c_a field) leads to a more frequent asymmetrical deformation (fig.15). Nevertheless, we also see fig.15 that even a well aged and very heterogeneous pellet leads to a a symmetric deformation in most of cases. This means that the final result does not depend only on statistics, but also on the real spatial distribution of the initial field c_a. The underlying process of localization can be well understood with fig. 11: at the beginning of plastic strain, a shear band forms in the pellet, but its position can be influenced by the local state of the material (non aged zones are softer) and therefore be closer to one of the ends of the pellet. The band then tends to move towards the center of the pellet, but the shape of the pellet at 0.6% total axial strain is still asymmetric. This proves that there is a deterministic chaos effect: small variations of local state may lead to great variations of the final shape of the sample. As a general result, we have shown that asymmetrical deformation results from the heterogeneity of ageing in the UO_2 pellet. This heterogeneity is a necessary condition but not a sufficient condition, as the deformation can be symmetrical even for an aged and heterogeneous pellet.

5 Conclusion

A study of previous experimental results showed that observed strain softening of UO_2 must result of an interaction between moving point defects and dislocations (also called ageing) rather than an initial lack of mobile dislocation followed by a fast multiplication, at it was before assumed. This hypothesis was confirmed by our simulations. Indeed, the ageing mechanism allows to develop a rather simple 1D model of UO_2 which well reproduces the different observed phenomena. This model can be applied to other ceramics or metals in which strain softening is also observed. The model was then extended to a 3D model and used to simulate a full pellet compressive test. The main result is that our model allows the strain to be localized in a special manner (asymmetrical localization of strain), provided that the initial material is not considered as perfectly homogeneous. We used the initial value

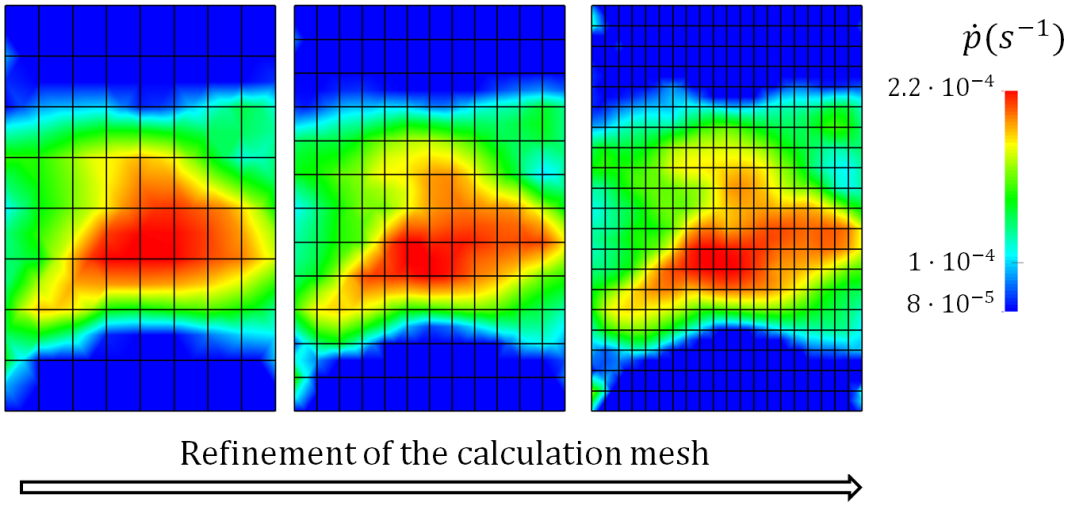

Figure 13: Illustration of mesh independence: the strain rate field (plotted at the exact same time for the same mechanical problem) converges when refining the calculation mesh

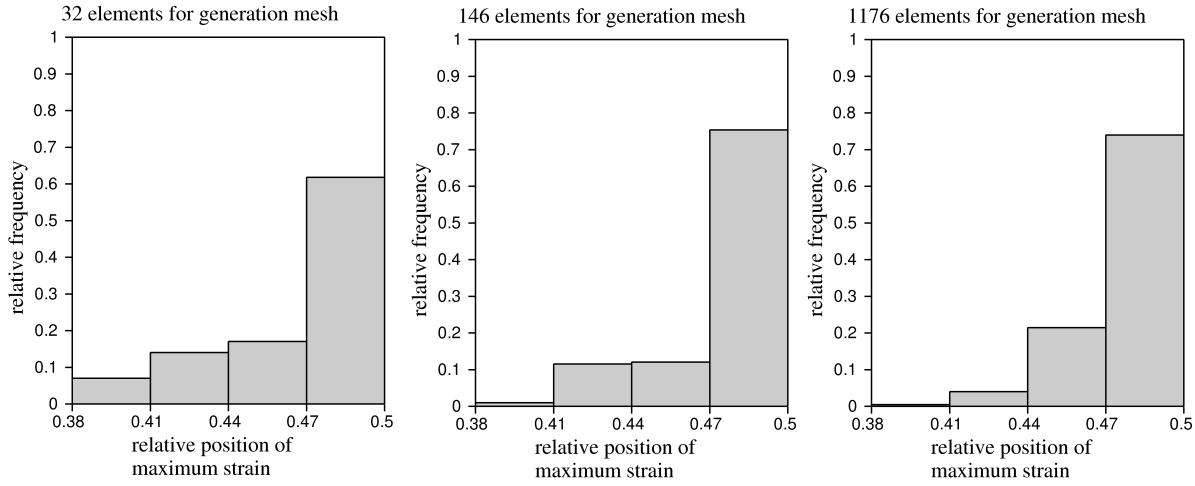

Figure 14: Effect of the refinement of the generation mesh on position of maximum strain plane, with given Gaussian distribution for c_a ($\mu = 3$, $s = 2$). A fine generation mesh does not allow very asymmetric shapes (right), whereas a coarse generation mesh does (left).

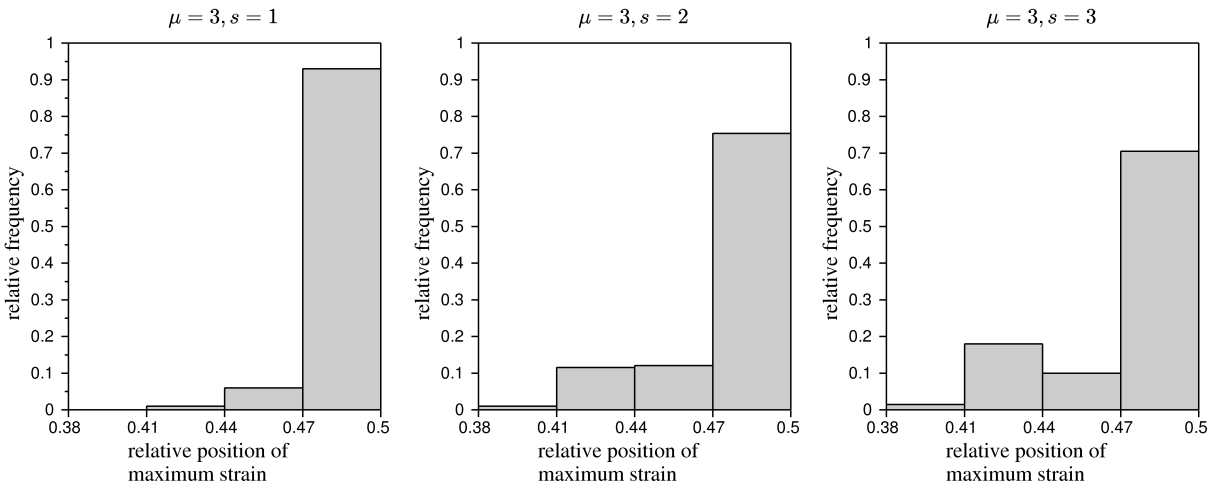

Figure 15: Effect of s (standard deviation of t^*) (with $\mu = 3$ constant) on position of maximum strain plane, with given generation mesh (146 elements). The relative frequency of asymmetric shapes (relative position of maximum strain far from 0.5) is growing with increasing s, i.e. heterogeneity.

of the relative ageing concentration to control this heterogeneity. Such strain localization is actually observed during compressive tests, and our model shows that this is due to the specific behavior of UO_2 at a certain temperature and strain rate range, when strain softening is strong and strain rate sensitivity is low. The physical nature of heterogeneity has not been formally identified though. Our study highlights the importance of accounting for an initial heterogeneity in the material to first avoid an artificial mesh dependence of the finite element study, and secondly to obtain the real shape of the deformed sample. Finally, it should be noted that only few different parameters had to be fitted to reproduce the whole mechanical behavior, including strain softening and variations with strain rate and temperature.

Acknowledgment

This work has been achieved in the framework of the PLEIADES project, financially supported by CEA (Commissariat à l'Énergie Atomique et aux Énergies Alternatives), EDF (Électricité de France) and AREVA.

References

[Armstrong and Irvine, 1964] Armstrong, W. and Irvine, W. (1964). Creep of urania base solid solutions. *Journal of nuclear materials*, 12:261–270.

[Armstrong et al., 1962] Armstrong, W., Irvine, W., and Martinson, R. (1962). Creep deformation of stoichiometric uranium dioxide. *Journal of Nuclear Materials*, 7:133–141.

[Bell and Bonfield, 1964] Bell, R. and Bonfield, W. (1964). The plastic deformation of germanium single crystals : yield and ideal easy glide. *Philosophical Magazine*, 9:9–36.

[Borst, 2001] Borst, R. d. (2001). Some recent issues in computational failure mechanics. *International Journal for Numerical Methods in Engineering*, 52(1-2):63–95.

[Brown and Pratt, 1963] Brown, M. and Pratt, P. (1963). Strain ageing in cdcl2-doped rock salt. *Philosophical Magazine*, 8:717–734.

[Bullough and Newman, 1970] Bullough, R. and Newman, R. (1970). The kinetics of migration of point defects to dislocations. *Report on progress in physics*, 33:101–148.

[Burton and Reynolds, 1973] Burton, B. and Reynolds, G. (1973). The influence of deviation from stoichiometric composition on the diffusional creep of uranium dioxide. *Acta Metallurgica*, 21:1641–1647.

[Chaboche et al., 2013] Chaboche, J.-L., Gaubert, A., Kanouté, P., A. Longuet, F. A., and Mazière, M. (2013). Viscoplastic constitutive equations of combustion chamber materials including cyclic hardening and dynamic strain aging. *International Journal of Plasticity*, 46:1–22.

[Christie and Williams, 1962] Christie, G. and Williams, J. (1962). The effect of small additions of yttria on the plasticity of uranium oxides at 940^{o}C. *Journal of nuclear materials*, 5:1–4.

[Cottrell and Bilby, 1949] Cottrell, A. and Bilby, B. (1949). Dislocation theory of yielding and strain ageing of iron. *Proc. Phys. Soc. A*, 62:49–62.

[Engelen et al., 2003] Engelen, R. A., Geers, M. G., and Baaijens, F. (2003). Nonlocal implicit gradient-enhanced elasto-plasticity for the modelling of softening behaviour. *International Journal of Plasticity*, 19(4):403–433.

[Estrin and Kubin, 1991] Estrin, Y. and Kubin, L. (1991). Plastic instabilities: phenomenology and theory. *Materials Science and Engineering A*, 137:125–134.

[Estrin and McCormick, 1991] Estrin, Y. and McCormick, P. (1991). Modelling the transient flow behaviour of dynamic strain ageing materials. *Acta Metallurgica et Materialia*, 39:2977–2983.

[F. Dherbey, 2002] F. Dherbey, F. Louchet, A. M. S. L. (2002). Elevated temperature creep of polycrystalline uranium dioxide: from microscopic mechanisms to macroscopic behaviour. *Acta Materialia*, 50:1495–1505.

[Fossati, 2012] Fossati, P. (2012). *Contribution à l'étude des propriétés mécaniques du combustible nucléaire : modélisation atomistique de la déformation du dioxyde d'uranium*. PhD thesis, Ecole Centrale Paris.

[Friedel, 1964] Friedel, J. (1964). *Dislocations*. Pergamon Press.

[Frost and Ashby, 1982] Frost, H. and Ashby, M. (1982). *Deformation-mechanism maps: the plasticity and creep of metals and ceramics*. Pergamon Press.

[Gallardo-Lopez et al., 2004] Gallardo-Lopez, A., Gomez-Garcia, D., Dominguez-Rodriguez, A., and Kubin, L. (2004). Portevin-le chatelier effect in Y2O3-ZrO2 single crystals. *Scripta Materialia*, 51:203–207.

[Gilman, 1961] Gilman, J. (1961). Mechanical behavior of ionic crystals. *Progress in Ceramic Science*, 1:146–199.

[Goretta and Routbort, 1986] Goretta, K. and Routbort, J. (1986). Dynamic strain aging and serrated flow in mno. *Journal of Materials Research*, 1:124–129.

[Guerin, 1973] Guerin, Y. (1973). *Etude par compression à hautes températures de la déformation plastique du bioxyde et du monocarbure d'uranium*. PhD thesis, Université Claude Bernard - Lyon.

[Guerin, 1975] Guerin, Y. (1975). Etude par compression à hautes températures de la déformation plastique du bioxyde d'uranium polycristallin. *Journal of Nuclear Materials*, 56:61–75.

[Harper, 1951] Harper, S. (1951). Precipitation of carbon and nitrogen in cold-worked alpha-iron. *Physical Review*, 83:709–712.

[Johnston, 1962] Johnston, W. (1962). Yield points and delay times in single crystals. *Journal of Applied Physics*, 33:2716.

[Keller et al., 1988a] Keller, R., Mitchell, T., and Heuer, A. (1988a). Plastic deformation in nonstoichiometric $UO_2 + x$ single crystals -i deformation at low temperatures. *Acta Metallurgica*, 36:1061–1071.

[Keller et al., 1988b] Keller, R., Mitchell, T., and Heuer, A. (1988b). Plastic deformation in nonstoichiometric $UO_2 + x$ single crystals -ii deformation at high temperatures. *Acta Metallurgica*, 36:1073–1083.

[Kronberg, 1957] Kronberg, M. (1957). Plastic deformation of single crystals of sapphire: basal slip and twinning. *Acta Metallurgica*, 5(9):507–524.

[Kubin and Estrin, 1990] Kubin, L. and Estrin, Y. (1990). Evolution of dislocation densities and the critical conditions for the Portevin-Le Chatelier effect. *Acta Metallurgica and Materialia*, 38:697–708.

[Kubin et al., 1992] Kubin, L., Estrin, Y., and Perrier, C. (1992). On static strain ageing. *Acta Metallurgica et Materialia*, 40:1037–1044.

[Lefebvre, 1976] Lefebvre, J. (1976). *Contribution à l'étude de la déformation plastique d'une céramique de structure fluorite : le bioxide d'uranium*. PhD thesis, Faculté des sciences de Poitiers.

[Lemaitre et al., 2009] Lemaitre, J., Chaboche, J.-L., Benallal, A., and Desmorat, R. (2009). *Mécanique des matériaux solides-3ème édition*. Hachette. com.

[Ling and McCormick, 1993] Ling, C. and McCormick, P. (1993). The effect of temperature on strain rate sensitivity in an Al-Mg-Si alloy. *Acta Metallurgica et Materialia*, 41:3127–3131.

[Martin, 1989] Martin, D. (1989). *High Temperature - High Pressure*, 21:13–24.

[Mazière and Dierke, 2012] Mazière, M. and Dierke, H. (2012). Investigations on the Portevin-Le Chatelier critical strain in an aluminum alloy. *Computational Materials Science*, 52:68–72.

[McCormick, 1988] McCormick, P. (1988). Theory of flow localisation due to dynamic strain ageing. *Acta Metallurgica*, 36:3061–3067.

[Mesarovic, 1995] Mesarovic, S. (1995). Dynamic strain aging and plastic instabilities. *Journal of the Mechanics and Physics of Solids*, 43:671–700.

[Michel et al., 2013] Michel, B., Nonon, C., Sercombe, J., Michel, F., and Marelle, V. (2013). Simulation of pellet-cladding interaction with the pleiades fuel performance software environment. *Nuclear Technology*, 182:124–137.

[Michel et al., 2008] Michel, B., Sercombe, J., Thouvenin, G., and Chatelet, R. (2008). 3D fuel cracking modelling in pellet cladding mechanical interaction. *Engineering Fracture Mechanics*, 75:3581–3598.

[Mitchell and Heuer, 2005] Mitchell, T. and Heuer, A. (2005). Dislocations and mechanical properties of ceramics. *Dislocations in solids*, 12:339–402.

[Mohamed and Soliman, 1982] Mohamed, F. A. and Soliman, M. S. (1982). On the creep behavior of uranium dioxide. *Materials Science and Engineering*, 53:185–190.

[Monerie and Gatt, 2006] Monerie, Y. and Gatt, J.-M. (2006). Overall viscoplastic behavior of non-irradiated porous nuclear ceramics. *Mechanics of Materials*, 38:608–619.

[Mura et al., 1961] Mura, T., Lautenschlager, E., and Brittain, J. (1961). Segregation of solute atoms during strain aging. *Acta Metallurgica*, 5:453–458.

[Nadeau, 1969] Nadeau, J. (1969). Dependence of flow stress on nonstoichiometry in oxygen-rich uranium dioxide at high temperatures. *Journal of the american ceramic society*, 52:1–8.

[Needleman, 1988] Needleman, A. (1988). Material rate dependence and mesh sensitivity in localization problems. *Computer Methods in Applied Mechanics and Engineering*, 67(1):69–85.

[Pacull, 2011] Pacull, J. (2011). *Modèle numérique micro-mécanique d'agrégat polycristallin pour le comportement des combustibles oxydes*. PhD thesis, Université de Provence - Aix-Marseille I.

[Peerlings et al., 2001] Peerlings, R., Geers, M., De Borst, R., and Brekelmans, W. (2001). A critical comparison of nonlocal and gradient-enhanced softening continua. *International Journal of Solids and Structures*, 38(44):7723–7746.

[Pijaudier-Cabot et al., 1988] Pijaudier-Cabot, G., Bažant, Z. P., and Tabbara, M. (1988). Comparison of various models for strain-softening. *Engineering computations*, 5(2):141–150.

[Poirier, 1980] Poirier, J. (1980). Shear localization and shear instability in materials in the ductile field. *Journal of Structural Geology*, 2:135–142.

[Quere, 1967] Quere, Y. (1967). *Défauts ponctuels dans les métaux*. Editions Masson.

[Sauter and Leclercq, 2003] Sauter, F. and Leclercq, S. (2003). Modeling of the non-monotonous viscoplastic behavior of uranium dioxide. *Journal of Nuclear Materials*, 322:1–14.

[Scott et al., 1959] Scott, R., Hall, A., and Williams, J. (1959). The plastic deformation of uranium oxides above 800^{o}C. *Journal of nuclear materials*, 1:39–48.

[Seltzer et al., 1971] Seltzer, M., Perrin, J., Clauer, A., and Wilcox, B. (1971). Review of creep behavior of ceramic nuclear fuels. *Reactor Technology*, 14:99–135.

[Srinivasan and Stoebe, 1973] Srinivasan, M. and Stoebe, T. (1973). Dynamic strain aging in magnesium oxide single crystals. *Materials Science and Engineering*, 12:87–93.

[Teodosiu, 1976] Teodosiu, C. (1976). A theory of finite elastoviscoplasticity of single crystals. *International Journal of Engineering Science*, 14:165–176.

[Tikhonovsky, 2001] Tikhonovsky, A. (2001). *Plastic deformation of cubic zirconia single crystals: The influence of the orientation of compression axis and yttria stabilizer content*. PhD thesis, Martin-Luther-Universitat Halle-Wittenberg.

[Vivant-Duguay, 1998] Vivant-Duguay, C. (1998). *Contribution à l'étude du fluage du dioxyde d'uranium, rôle des activateurs de croissance cristalline*. PhD thesis, Institut National des Sciences Appliquées de Lyon.

[Wachtman and Maxwell, 1954] Wachtman, J. and Maxwell, I. (1954). Plastic deformation of ceramic-oxide single crystals. *Journal of the American Ceramic Society*, 37(7):291–299.

[Yust and McHargue, 1969] Yust, C. and McHargue, C. (1969). Dislocation substructures in deformed uranium dioxide single crystals. *Journal of nuclear materials*, 31:121–137.